arXiv:0811.4540v1 [physics.ins-det] 27 Nov 2008

# Monolithic Pixel Sensors in Deep-Submicron SOI Technology with Analog and Digital Pixels

Marco Battaglia [a,b], Dario Bisello [c], Devis Contarato [a,*], Peter Denes [a], Piero Giubilato [a,c],
Lindsay Glesener [b], Serena Mattiazzo [c], Chinh Vu [a]
[a] *Lawrence Berkeley National Laboratory, Berkeley, CA 94720, USA*
[b] *Department of Physics, University of California at Berkeley, CA 94720, USA*
[c] *Dipartimento di Fisica, Università di Padova and INFN, Sezione di Padova, I-35131 Padova, Italy*

---

**Abstract**

This paper presents the design and test results of a prototype monolithic pixel sensor manufactured in deep-submicron fully-depleted Silicon-On-Insulator (SOI) CMOS technology. In the SOI technology, a thin layer of integrated electronics is insulated from a (high-resistivity) silicon substrate by a buried oxide. Vias etched through the oxide allow to contact the substrate from the electronics layer, so that pixel implants can be created and a reverse bias can be applied. The prototype chip, manufactured in OKI 0.15 $\mu$m SOI process, features both analog and digital pixels on a 10 $\mu$m pitch. Results of tests performed with infrared laser and 1.35 GeV electrons and a first assessment of the effect of ionising and non-ionising doses are discussed.

*Key words:* Monolithic pixel sensor; SOI; CMOS technology; Particle detection

---

## 1. Introduction

Silicon on insulator (SOI) technology allows the fabrication of CMOS integrated circuits on a thin silicon layer which is electrically insulated from the rest of the silicon wafer by means of a buried-oxide (BOX). The small active volume and low junction capacitance ensure latch-up immunity, low-threshold operation and low noise, thus favouring high-speed, low power designs. The isolation of the electronics from a high-resistivity substrate, together with the capability of contacting the latter by means of vias through the BOX, allows the design of monolithic pixel sensors for radiation detection which offer many advantages with respect to devices fabricated in a standard bulk CMOS process. A full CMOS circuitry can be integrated in each pixel, thus allowing for complex digital designs, while the depletion of the sensor wafer results in an improved charge collection efficiency. Furthermore, present-day deep-submicron processes allow for a high miniaturisation and integration of complex architectures in devices with small pixel pitch. A proof of principle of the concept was obtained by the SUCIMA Collaboration, using a 3 $\mu$m process from IET, Poland [1,2,3]. The recent availability of deep-submicron, fully-depleted SOI CMOS process from OKI, Japan [4] opened up the possibility of fabricating SOI monolithic pixel sensors with small pixel pitches and larger integration capabilities. The process features a full CMOS circuitry implanted on a 40 nm thin Si layer on top of a 200 nm thick BOX. The thickness of the CMOS layer is small enough for the layer to be fully depleted at typical operational voltages. The sensor substrate is 350 $\mu$m thick and has a resistivity of 700 $\Omega$·cm. The adequacy of the OKI process for the fabrication of monolithic pixel sensors was first demonstrated at KEK in 2006 [5]. A first prototype sensor designed at LBNL was manufactured in 2007 in the OKI 0.15 $\mu$m FD process. The chip features both analog and digital pixels. The first results on the detection of 1.35 GeV electrons with the analog pixels have already been reported in [6]. In this paper we discuss further tests of the analog pixels to determine the charge sharing and the cluster position resolution using an IR laser and the first results of the characterisation of the digital pixels using 1.35 GeV electrons form the BTS beam at the LBNL Advanced Light Source (ALS).

---

[*] Corresponding author. Address: Lawrence Berkeley National Laboratory, 1 Cyclotron Road, Berkeley, CA 94720 (USA). E-mail: `DContarato@lbl.gov` (Devis Contarato).

## 2. Chip Design, Readout and Data Analysis

The first prototype sensor, named LDRD-SOI-1, was manufactured in 2007 in the OKI 0.15 $\mu$m FD process [6]. The chip features an array of 160×150 pixels on a 10 $\mu$m pitch, subdivided into two analog sections and one digital section, each comprising 160×50 pixels (see Figure 1). The two analog sections implement a simple 3-transistor (3T) architecture based on thin-oxide 1.0 V transistors and thick-oxide 1.8 V transistors. The digital pixels operates at a bias $\mathrm{V_{DD}}$=1.8 V and implement an in-pixel latch triggered by a comparator connected to an adjustable voltage threshold which is common to the whole matrix. No amplifier is present in the digital pixels, so that static power dissipation is avoided, the pixel being active only when the latch is triggered.

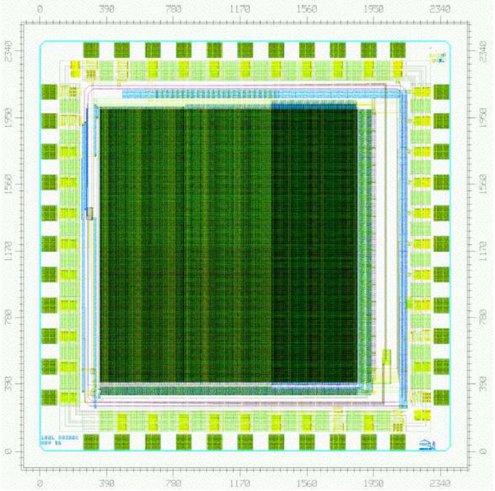

Fig. 1. Layout of the LBNL LDRD-SOI1 prototype pixel chip.

A potential limitation of the SOI technology comes from the back-gating effect. The reverse bias of the silicon substrate increases the potential at the silicon surface, so that the buried oxide acts as a second gate for the CMOS electronics on top, typically causing a shift in the transistor thresholds as a function of the increasing depletion voltage. The effect could be evaluated from single transistor test structures implemented at the chip periphery. Tests of complementary *p*-type and *n*-type MOSFETs showed a threshold shift of ∼200 mV for a substrate bias of 15 V. TCAD simulations performed with the Synopsys `Taurus Device` package have shown that the inclusion of a floating *p*-type guard-ring around each pixel is beneficial in keeping the field low in the area between diode implants, thus limiting potential back-gating effects on the CMOS electronics on top of the buried oxide. A series of floating and grounded guard-rings was also implemented around the pixel matrix and around the peripheral I/O electronics.

Each 8000-pixel analog section is read out independently by a custom FPGA-based readout board with 14-bit ADCs. Pixels are clocked at 6.25 MHz, with an integration time of 1.382 ms for the analog pixels, while the integration time for the digital pixels is tunable. Correlated Double Sampling (CDS) is performed for the analog pixels by acquiring two frames of data without resetting the pixels in-between the readings and subtracting the first frame from the second. The binary output of the digital pixels is simply buffered through the FPGA to the DAQ board digital outputs connected to a National Instruments PCI 6533 digital acquisition board installed on the PCI bus of a control PC. Data is processed on-line by a LabView-based program and converted into the `lcio` format [7]. Offline data analysis is based on a set of dedicated processors developed in the `Marlin` C++ reconstruction framework [8], which perform data quality and event selection, clusterisation and hit position reconstruction.

## 3. 3T Analog Pixels

The response of the analog sections has been first tested with a 1060 nm IR laser focused to a ≃20 $\mu$m spot, and measuring the pulse height in a 5×5 pixel matrix, centred around the laser spot centre. For depletion voltages $V_d$ <10 V, the measured signal was found to increase proportionally to $\sqrt{V_d}$, as expected from the increase of the depletion region thickness. For larger $V_d$ values, the signal was found to first saturate and then decrease for $V_d$ ≥15 V, suggesting an effect due to the back-gating of the MOSFETs in the pixel and/or in the output buffer. Such effect appears in the 1.0 V transistor pixels at lower $V_d$ values compared to the 1.8 V transistor pixels (see Figure 2).

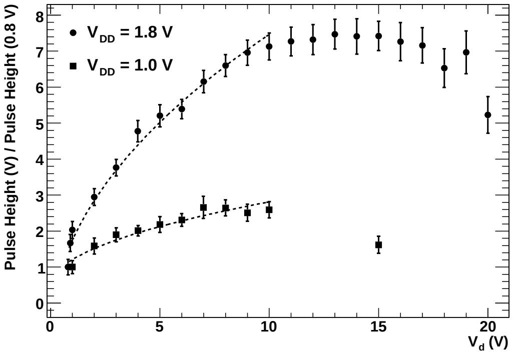

Fig. 2. Cluster pulse height normalised to that measured at $V_d$ = 0.8 V for a focused 1060 nm laser spot as a function of the substrate bias, $V_d$ (from [6]).

The spatial resolution of the analog pixels has been determined by focusing the 1060 nm laser beam to a ≃5 $\mu$m Gaussian spot and performing pixel scans by shifting the spot along single pixel rows in steps of 1 $\mu$m using a stepping motor with a positioning accuracy of 0.1 $\mu$m. The laser hit position is reconstructed from the centre of gravity of the pixel cluster and the resolution is obtained from the spread of the reconstructed cluster position for the events taken at each point in the scan (see Figure 3). The laser intensity is varied in order to obtain different S/N values, from values below that observed for 1.35 GeV electron sig-

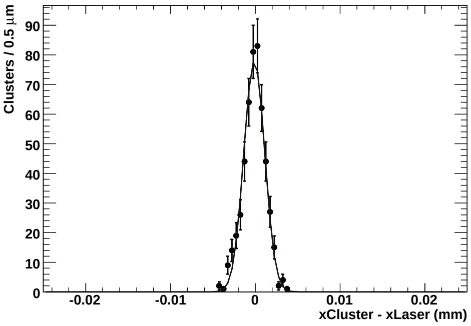

Fig. 3. Distribution of the differences between the position of a 5 $\mu$m laser spot and the reconstructed cluster position in the SOI analog pixels. The measurement has been performed with a S/N of 20 and a depletion voltage $V_d$ = 7 V. The r.m.s. of the fitted Gaussian function is 1.2 $\mu$m.

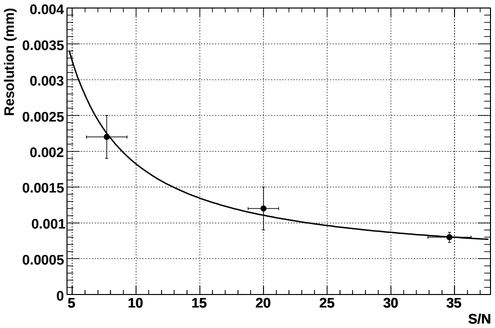

Fig. 4. Single point resolution as a function of the S/N ratio obtained from scans of the analog pixels performed with a 1060 nm laser focused to a 5 $\mu$m spot, for a depletion voltage $V_d$=7 V. Data points represent the mean of the distribution of the differences between the laser spot position and reconstructed cluster position, the error bars give their r.m.s. values. The overlayed function shows the expected $(\mathrm{S/N})^{-1}$ scaling.

nals (see next section) up to S/N $\simeq$ 35. Results obtained for different S/N values and for a depletion voltage $V_d$=7 V are shown in Figure 4: pixels with 10 $\mu$m pitch have a single point resolution of 1 $\mu$m for a S/N ratio of 20 or larger and the measured resolution scales as the inverse of the S/N, as expected.

The response of the analog pixels to high-momentum charged particles has been tested on the 1.35 GeV electron beam extracted from the booster of the LBNL Advanced Light Source (ALS) and results have been reported in detail in [6]. The pixel multiplicity in a cluster was found to slightly decrease with increasing depletion voltage, while the cluster pulse height increased up to 10 V. At 15 V the cluster signal and the efficiency of the chip decreased, as observed in the laser tests. A signal-to-noise ratio up to 15 was measured with the 1.8 V analog section for 5 V$\leq V_d \leq$15 V.

## 4. Digital Pixels

The response of the digital pixels to high-momentum charged particles has also been tested on the ALS 1.35 GeV electron beam. The digital pixels are triggered directly by the 1 Hz booster extraction signal and are latched and read out after allowing an integration time of 10 $\mu$s. Data have been taken at different depletion voltages, up to 35 V. The depletion voltages used correspond to an estimated depletion thickness from 56 $\mu$m for $V_d$ = 15 V, up to 80 $\mu$m for $V_d$ = 30 V.

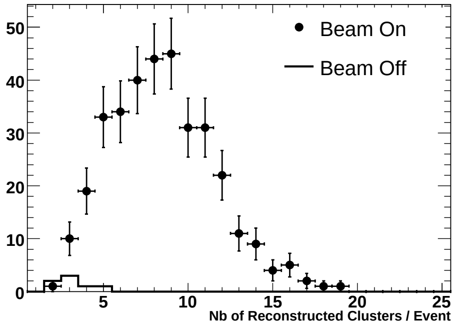

Fig. 5. Hit multiplicity for 1.35 GeV $e^-$s for the digital pixels at a depletion voltage of 30 V (markers with error bars). The distribution of fake hits reconstructed in the absence of beam (continuous line) is also shown for comparison.

For each run the first 100 events have been used to map the noisy pixels. Pixels giving a signal for more than 25 events have been flagged as noisy and masked for the rest of the run. Figure 5 shows the hit multiplicity observed in the digital pixels for events taken with and without beam, for $V_d$=30 V. A clear excess of hits can be seen in presence of beam. The small background obtained in the absence of beam is due to noisy pixels which survive the cluster reconstruction cuts applied in the data analysis. In order to evaluate the effect of $V_d$ on the particle response, dedicated data runs have been taken at low beam intensity with a single detector reference plane, located 2 cm upstream from the LDRD-SOI1 sensor. The reference plane consists of a 50 $\mu$m-thin MIMOSA-5 CMOS pixel sensor. The MIMOSA-5 chip was developed by IPHC, Strasbourg (France) [9,10] and features a 1.7×1.7 cm$^2$ active area with more than 1 Million pixels on a 17 $\mu$m pitch, arranged in four independent sectors. The performance of thin MIMOSA-5 sensors, the readout system and analysis procedures adopted are presented in details in [11,12]. The particle flux in the area corresponding to the active region of the LDRD-SOI1 digital pixel sector has been monitored from the number of electron hits reconstructed on the reference plane, on a run by run basis. We compute the average number of hits per spill on the digital pixels, for different depletion voltages, and correct it for the relative change of the beam intensity, as determined by the reference plane. These changes are in the range of 5-40%, for the runs of interest. Results are summarized in Table 1. Signals from beam particles are observed on the digital section of the chip by applying a depletion voltage $\geq$ 20 V, while the analog pixels stop functioning properly above $\simeq$ 15 V. This can be explained by considering that the analog threshold of the in-pixel comparators is affected by back-gating, while the digital circuitry in each pixel is only active when triggered, i.e. for times much shorter compared to the analog pixels. At the same time, larger substrate voltages are needed to obtained large enough signals to be above threshold. These two effects seem to combine giving the best particle detection capabilities for $\simeq$ 25 V. Using the particle flux reconstructed on the reference layer and its efficiency, as obtained from simulation [12], we estimate the efficiency of the SOI digital pixels to be of the order of 0.3 to 0.5 for 20 V$\leq V_d \leq$35 V.

| $V_d$ **(V)** | $\frac{Nb.Clusters}{Spill}$ **beam on** | $\frac{Nb.Clusters}{Spill}$ **beam off** | **<Nb Pixels> in Cluster** |
|---|---|---|---|
| 20 | 3.7±0.1 | 0.02 | 1.78 |
| 25 | 5.3±0.1 | 0.03 | 1.32 |
| 30 | 4.7±0.1 | 0.03 | 1.26 |
| 35 | 4.2±0.1 | 0.02 | 1.14 |

Table 1
Summary of beam test results obtained with 1.5 GeV electrons on the digital pixels. The average number of clusters per beam spill recorded with beam on and beam off and the average pixel multiplicity in a cluster are given for different values of $V_d$. The number of cluster per spill is corrected by changes in the beam intensity, obtained from the reference plane.

Data could be taken up to depletion voltages $V_d$=35 V, however with a much decreased counting rate. The average number of pixels in a cluster was found to decrease from 1.8 to 1.1 for $V_d$ increasing from 20 V to 35 V, consistently with an increased electric field in the detector substrate, as observed also for the analog pixels.

## 5. Radiation Hardness Tests

The SOI technology is expected share the intrinsic radiation tolerance of deep-submicron electronics and the capability of sustaining significant non-ionising doses of high resistivity Si. However, the thick buried oxide may be sensitive to ionising doses, which lead to positive charge trapping and consequently to an increase of the back-gate potential.

A preliminary assessment of the effect of ionising radiation on single transistors and of non-ionising radiation on the analog pixels has been obtained. Irradiations were performed at the BASE Facility of the LBNL 88-inch Cyclotron [13]. The first test was performed with 30 MeV protons on single transistors. The chip was mounted on the beam behind a 1-inch diameter collimator, and the terminals of two test transistors (one $p$-MOSFET and one $n$-MOSFET) were connected to a semiconductor parameter analyser so that the transistor characteristics could be measured in-between irradiation steps. During the irradiation steps, the transistor terminals were kept grounded. The irradiation was performed with a flux of $\sim 6\times10^7$ p/cm$^2$s, up to a total fluence of $2.5\times10^{12}$ p/cm$^2$, corresponding to a total dose of ~600 kRad. Figure 6 shows the variation in the threshold voltage for the $n$-MOS test transistor as a function of the proton fluence. An initial substrate voltage $V_d$=5 V was used, but after a fluence of about $1\times10^{12}$ p/cm$^2$ the transistor characteristics could not be properly measured, and a reduced substrate bias of $V_d$=1 V needed to be applied in order to recover the transistor characteristics. We interpret this effect as due to radiation-induced charge build-up in the buried oxide which effectively increases back-gating. The total threshold variation is indeed significant (~100 mV) also for a low substrate bias (i.e. $V_d$=1 V); the effect is much larger than what would be expected at such doses from radiation damage in the transistor thin gate oxide. Similar results were found on the $p$-MOS test transistor. The effect of non-ionising radiation has been studied exposing the LDRD-SOI1 detector chip to neutrons produced from 20 MeV deuteron breakup on a thin target at the LBNL 88-inch cyclotron [14]. The detector chip was located 8 cm downstream from the target and activation foils were placed just behind it to monitor the fluence. Deuteron breakup produces neutrons on a continuum spectrum from $\sim$ 1 MeV up to $\sim$ 14 MeV. A beam current of 800 nA was used, corresponding to an estimated flux at the chip position of $\simeq 4\times10^8$ $n$ cm$^{-2}$ s$^{-1}$. The measured $\gamma$ activity on the foils corresponds to a total fluence of $1.2\times10^{13}$ $n$ cm$^{-2}$. The noise of the sensor has been

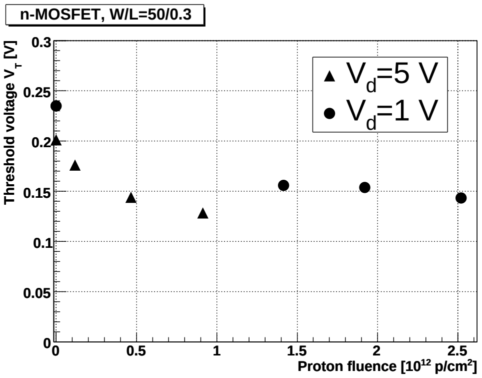

Fig. 6. Threshold voltage for a 1.0 V $n$-MOS test transistor with $W/L$=50/0.3 as a function of 30 MeV proton fluence for depletion voltages $V_d$=1 V and $V_d$=5 V.

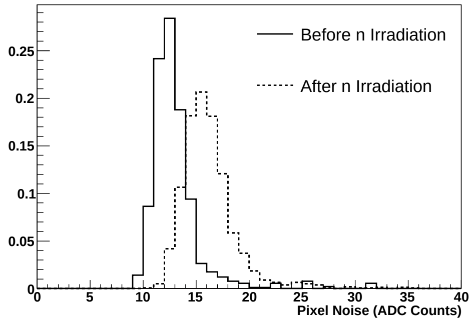

Fig. 7. Distribution of the noise of the analog pixels before (continuous line) and after (dashed line) irradiation with $1.2\times10^{13}$ $n$ cm$^{-2}$ for $V_d$ = 10 V. The histogram are normalised to unit area for comparison.

measured before and after the irradiation as a function of the depletion voltage, $V_d$. The detector is still functional after irradiation but we observe an increase of noise, which varies from +25 %, for $V_d = 5$ V, to +52 %, for $V_d = 20$ V, at room temperature (see Figure 7). We interpret this increase as due to leakage current. The pixel noise of the irradiated chip has therefore been measured, for $V_d = 10$ V, as a function of the operational temperature, $T$, in the range -5 °C $< T <$ +20 °C. At temperatures below +5 °C, the noise level measured before irradiation is recovered.

## 6. Conclusions and Outlook

A prototype monolithic pixel sensor including both analog and digital pixel cells has been designed and produced in OKI SOI technology, which combines deep-submicron CMOS electronics and a high resistivity substrate in the same device. The response of the prototype chip has been studied using both focused laser beams and the 1.35 GeV $e^-$ beam at the LBNL ALS. Both the analog and digital pixels were found to be functional. A S/N ratio of 15 has been obtained with the electron beam on the analog pixels up to depletion voltages $V_d$=15 V, and a single point resolution of $\simeq 1$ $\mu$m has been estimated using measurements performed with a narrowly focused IR laser beam. The digital section of the chip could be operated at higher depletion voltages compared to the analog part, as the digital circuitry in the pixels appears to be less affected by back-gating. Total ionising dose tests performed on single transistor test structures hint at the build-up of charge trapped in the buried oxide which enhance the effect of back-gating of the CMOS electronics. A moderate increase of the pixel noise from exposure to $10^{13}$ $n$ cm$^{-2}$ has been observed. These results establish the feasibility of monolithic pixel sensors in SOI technology, which is of great interest for the possibility to implement complex readout architectures combined with a high-resistivity, depleted substrate ensuring faster charge collection and larger signals, compared to bulk CMOS pixel sensors. Potential applications of this technology range from vertex tracking in high-energy physics experiments to soft X-ray detection at synchrotron facilities and fast nano-imaging imaging for beam diagnostics and monitoring. A second prototype chip, implementing digital pixels with in-pixel charge storage and correlated double sampling and fast readout has been recently fabricated in OKI 0.20 $\mu$m FD SOI process and is currently under test.

Acknowledgements This work was supported by the Director, Office of Science, of the U.S. Department of Energy under Contract No. DE-AC02-05CH11231. We thank the staff of the LBNL Advanced Light Source and 88-inch Cyclotron for their assistance and for the excellent performance of the machines.

## References

[1] J. Marczewski et al., Nucl. Instrum. Meth. A **549** (2005) 112.

[2] J. Marczewski et al., Nucl. Instrum. Meth. A **560** (2006) 26.

[3] H. Niemiec et al., Nucl. Instrum. Meth. A **568** (2006) 153.

[4] OKI Electric Industry Co. Ltd., Japan. `http://www.oki.com`

[5] T. Tsuboyama et al., Nucl. Instrum. Meth. A **582** (2007) 861.

[6] M. Battaglia et al., Nucl. Instrum. Meth. A **583** (2007) 526. [arXiv:0709.4218 [physics.ins-det]].

[7] F. Gaede *et al.* in the *Proc. of 2003 Conf. for Computing in High-Energy and Nuclear Physics* (CHEP 03), La Jolla, California, 24-28 Mar 2003, pp TUKT001, [arXiv:physics/0306114].

[8] F. Gaede, Nucl. Instrum. Meth. A **559** (2006) 177.

[9] Yu. Gornushkin *et al.*, Nucl. Instrum. and Meth. A **513** (2003) 291.

[10] G. Deptuch, Nucl. Instrum. and Meth. A **543** (2005) 537.

[11] M. Battaglia *et al.*, Nucl. Instrum. Meth. A **579** (2007) 675.

[12] M. Battaglia *et al.*, Nucl. Instrum. Meth. A **593** (2008) 292 [arXiv:0805.1504 [physics.ins-det]].

[13] M.A. McMahan, Nucl. Instrum. Meth. B **241** (2005) 409

[14] M.A. McMahan, Nucl. Instrum. Meth. B **261** (2007), 974.